# Intrinsic superstatistical components of financial time series

Călin Vamoş and Maria Crăciun

"T. Popoviciu" Institute of Numerical Analysis, Romanian Academy, P.O. Box 68, 400110 Cluj-Napoca, Romania

Received: date / Revised version: date

**Abstract.** Time series generated by a complex hierarchical system exhibit various types of dynamics at different time scales. A financial time series is an example of such a multiscale structure with time scales ranging from minutes to several years. In this paper we decompose the volatility of financial indices into five intrinsic components and we show that it has a heterogeneous scale structure. The small-scale components have a stochastic nature and they are independent 99% of the time, becoming synchronized during financial crashes and enhancing the heavy tails of the volatility distribution. The deterministic behavior of the large-scale components is related to the nonstationarity of the financial markets evolution. Our decomposition of the financial volatility is a superstatistical model more complex than those usually limited to a superposition of two independent statistics at well-separated time scales.

**PACS.** 89.65.Gh Economics; econophysics, financial markets, business and management – 05.45.Tp Time series analysis – 05.70.Ln Nonequilibrium and irreversible thermodynamics

## 1 Introduction

In the last two decades the physicists have become more and more interested in complex systems with hierarchical structure extending over many scales [1]. They are modeled by graphs including modules of different sizes which are grouped in a hierarchical manner [2]. Some of the most known examples of hierarchical multiscale systems are the financial markets [3]. Their time scales range continuously from minutes, where the market makers act, up to several years, intervals characteristic for investment funds. All these investors interact with each other. Asset prices are also influenced by many exterior economic and financial factors with even larger time scales (see for example Chap. 9 in [4]).

The statistical mechanics of such complex systems with a hierarchy of temporal or spatial scales is given by a superposition of several statistics, known as superstatistics [5,6]. The simplest form of the superstatistical model has only two separate scales with independent random dynamics. For example, the small-scale dynamics may describe a system in local thermodynamical equilibrium with a Boltzmann-Gibbs factor $e^{-\beta E}$, where $E$ is the system energy. If the intensive parameter $\beta$ slowly fluctuates at much larger scales, then the statistics of the whole system is given by an effective Boltzmann factor as a mixture of the microscopic statistics

$$F(E) = \int f(\beta) e^{-\beta E} d\beta, \qquad (1)$$

where $f(\beta)$ is the probability distribution function (pdf) of the parameter $\beta$. The resulting statistics generally have

non-Gaussian properties with heavy tails [5]. The essential supposition in this approach is the independence of the two scales, not their number. If there are several independent time scales, the integral in Eq. (1) is replaced by a multiple integral [7].

Many complex systems in various areas of science have been successfully modeled by this simple superstatistical model: turbulence, astrophysics, quantitative finance, climatology, random networks, medicine, etc. [8]. Remarkable results are obtained when the local equilibrium hypothesis holds as, for example, in turbulence [9]. But for biological or social systems this hypothesis is unlikely to stand all the time and then the global pdf is no more a simple integral as in Eq. (1) because we have to take into account the interactions between different time scales. In this paper we show that in most of the time the random small-scale fluctuations of the financial volatility have an independent evolution, but they become synchronized during financial crashes. Therefore a financial market seems to be a more complex system than a statistical system in local equilibrium in a slowly evolving environment.

A time series generated by such a complex system contains in a compressed form all the intricacies of its complex evolution. Hence one needs special algorithms to identify, separate, and analyze the evolution at different scales of a complex multiscale time series [10]. Usually the spectral analysis is realized in a nonadaptive manner, the time series being projected on a predetermined frequency grid, most often equidistant. This is the case even with the most popular multiresolution analysis supplied by the wavelet decomposition [11].

A better approach would be a data-driven numerical algorithm which should separate several intrinsic spectral components arranged in an increasing hierarchy of frequencies. For a correct characterization of the dynamics over different time scales, an essential issue is the proper separation of time scales between the intrinsic components. Otherwise, we risk to assign to a specific time scale a mixture of unrelated dynamics. The only algorithm known to us which adapts to the characteristics of nonlinear and nonstationary time series is the empirical mode decomposition (EMD) method [12]. But the EMD components are not constrained with respect to their spectral overlapping.

In this paper we present a numerical algorithm which is not only adaptive, but also decomposes a complex multiscale time series into several intrinsic components with minimum spectral superposition. Our decomposition algorithm is based on the condition that the spectral width of each intrinsic component should be minimum and disjoint from that of the neighboring components. Our decomposition algorithm allows us to show that the financial volatility contains a hierarchy of time scales with a heterogeneous scale structure and different dynamical properties. The small-scale intrinsic components have a random nature while the large-scale intrinsic components have a deterministic behavior rendering the financial time series nonstationary.

## 2 Financial volatility time series

The basic quantity in quantitative finance is the logreturn defined as $r_n = \log(S_{n+1}/S_n)$, where $\{S_n, 1 \leq n \leq N+1\}$ are the prices of a financial asset. The basic properties of daily financial returns, the so-called stylized facts [13], are captured by the heteroscedastic model

$$r_n = v_n z_n, \qquad (2)$$

where $\{z_n\}$ is a Gaussian white noise with zero mean and unit variance and $\{v_n\}$ is a stochastic process called volatility with strictly positive values and independent of $\{z_n\}$ [14]. It is a particular case of the superstatistical model. If in Eq. (2) the volatility fluctuates much slower than the Gaussian noise, then the pdf of the logreturns is a mixture of Gaussians

$$F(r) = \int_0^\infty \frac{1}{(2\pi)^{1/2}v} \exp\left(-\frac{r^2}{2v^2}\right) f(v)dv, \qquad (3)$$

where $f(v)$ is the pdf of the volatility. The superstatistical model was successfully applied to several financial time series [15–18].

In Fig. 1(a) we plot the daily returns computed from the daily closing values of the S&P500 index from 1 January 1950 to 28 July 2012, a time series containing $N = 15724$ values. The volatility is obtained as the moving average (MA) of the absolute values of the logreturns [19]

$$v_n = \frac{1}{2K+1} \sum_{k=-K}^{K} |r_{n+k}|, \qquad (4)$$

where $K$ is the semilength of the averaging window and $K < n \leqslant N - K$. If $n \leqslant K$ ($n > N - K$), then the average is taken over the first $n + K$ (the last $N - n + K + 1$) values of $|r_n|$. The properties of this MA with normalized padding with zero at boundaries are analyzed in [20].

Figures 1(b) and (c) show the volatility and the noise $z_n = r_n/v_n$ estimated by an MA with $K = 3$ such that the small scale fluctuations of the volatility are preserved [17,18]. The estimated noise is Gaussian [Fig. 2(a)] but it is uncorrelated only for lags larger than 5 days [Fig. 2(b)] due to the spurious correlations introduced by the MA (see Appendix B in [20]). Then the estimated volatility is accurate only for time scales larger than 5 days and its intrinsic components may be determined only for these time scales.

To measure the components spectral width we need a flexible local measure suited for a complex time series. Time scales are usually defined as the periods of the constant-amplitude trigonometric components of the Fourier decomposition. Instead of such a global averaged description, we use the characteristic times defined as the spacings between successive local extrema of the time series, also equal to the lengths of its monotonic segments [12]. For an arbitrary time series we denote the characteristic times by $\lambda_j$, $1 \leq j \leq J$. In the simplest cases, the set $\{\lambda_j\}$ supplies a full description of the time series spectrum. For instance, a harmonic oscillation has all $\lambda_j$ equal to half the oscillation period.

The situation is more complex in the case of a noisy time series. The characteristic times distribution is dominated by the small-scale fluctuations of the noise and it does not distinguish the large-scale variations possibly existing in the time series. Quantitatively, a time series cannot contain monotonic variations smaller than $\lambda_{\min} = \min\{\lambda_j\}$, but there may exist components with monotonic variations lasting longer than $\lambda_{\max} = \max\{\lambda_j\}$. For instance, the histogram of the characteristic times of the estimated volatility of the S&P500 index is dominated by fluctuations with characteristic times smaller than $\lambda_{\max} = 14$ [Fig. 2(c)], which are much smaller than the characteristic times of the large-scale components of the volatility. Our goal is to decompose the volatility into a hierarchy of superstatistical components with characteristic times larger than 5 business days, such that the intervals $I_\lambda = [\lambda_{\min}, \lambda_{\max}]$ associated to them should be disjoint.

## 3 Decomposition algorithm

We will decompose the volatility into superstatistical components $v_n^{(c)}$

$$v_n = V v_n^{(1)} v_n^{(2)} ... v_n^{(C)} w_n^{(C)}, \qquad (5)$$

where $V$ is the mean volatility and $w_n^{(C)}$ are the volatility residuals of order $C$. For several reasons, this is a generalization of the superstatistical model with two independent scales described in the previous section. First, the number of the time scales is not limited to two. If they are independent, then the integral in Eq. (3) is replaced by a multiple
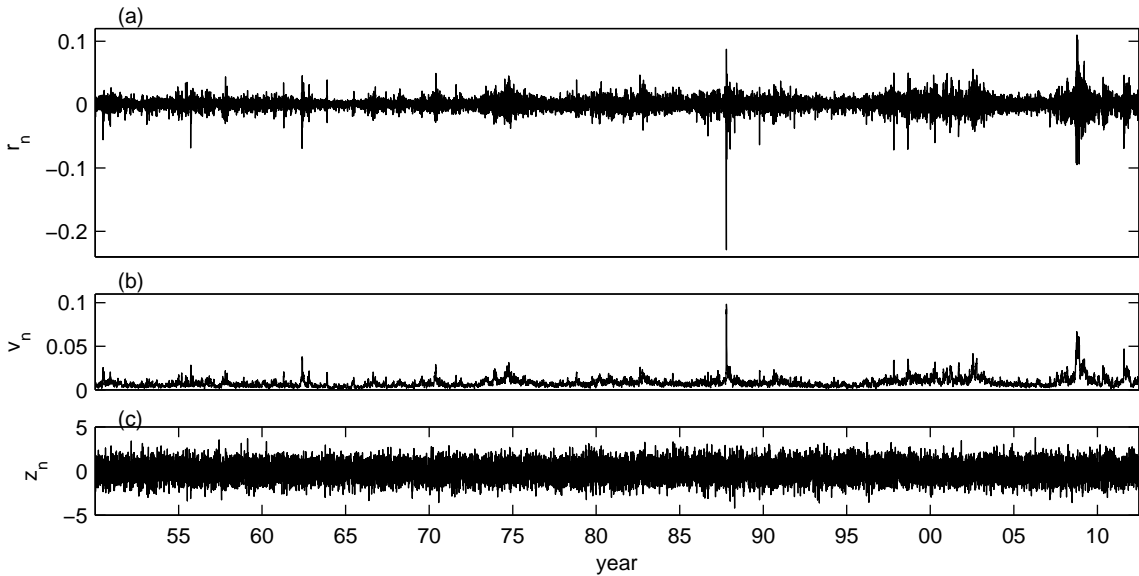
**Fig. 1.** The logreturns $\{r_n\}$ (a), the estimated volatility $\{v_n\}$ (b), and the estimated white noise $\{z_n\}$ (c) of the S&P500 index.
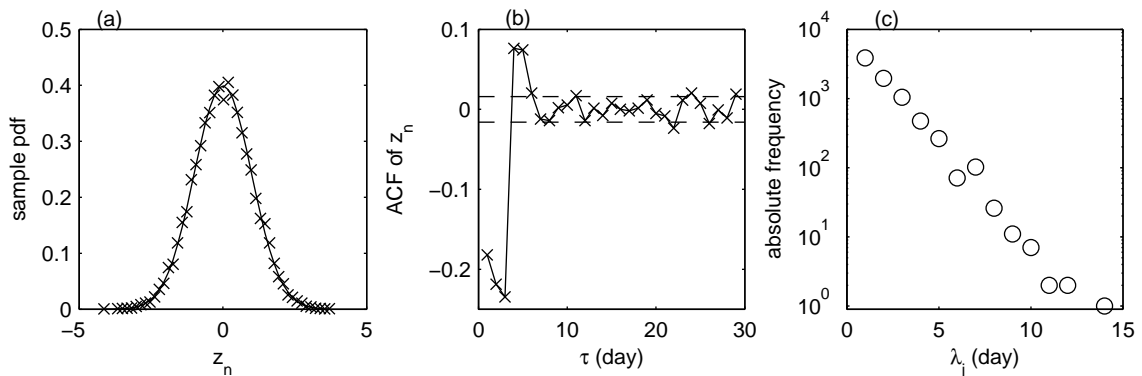


**Fig. 2.** (a) The sample pdf of the estimated noise compared with a Gaussian. (b) The autocorrelation function of the estimated noise and its 95% confidence interval (dashed lines). (c) The histogram of the number of the monotonic segments of the estimated volatility as a function of their lengths.

integral [7]. Here we allow that the evolutions at different scales may be correlated and then the global pdf cannot be computed as an integral. Also, the residuals $w_n^{(C)}$ may be non-Gaussian. Finally, we make no assumption on the nature of the components (deterministic or random). In this section we describe the numerical decomposition algorithm and in the next section we exemplify how it works in the case of the S&P500 index.

Similar to the SiZer algorithm [21], we compute the components $v_n^{(c)}$ by successive smoothings, which gradually eliminate the variations with the largest characteristic times from the previous component. Let us assume that the first $c$ components have been computed. We denote by $I_\lambda^{(c)}$ the interval containing its characteristic times $\lambda_j^{(c)}$ ($1 \le j \le J^{(c)}$) equal to the lengths of the monotonic segments. The next component is determined such that the interval $I_\lambda^{(c+1)}$ should have minimum width and should be

as close as possible to the previous interval $I_\lambda^{(c)}$. In this way the time scales of the components are not predetermined, but they are controlled by data themselves and the resulting algorithm has an adaptive nature.

For smoothing we use the repeated central MA (RCMA) with normalized padding with zero at boundaries (Chap. 4 in [20]) obtained by repeating the smoothing (4) several times. Its parameters are the semilength $K$ of the averaging window and the number of repetitions $i$ of the MA. Roughly the same smoothing is realized by averaging many times with a small $K$ or several times with a large $K' > K$ [20]. Therefore we maintain $i$ between 15 and 20 repetitions and we vary mainly the semilength $K$ from one component to the next.

We denote by $\{u_n^{(c+1;1)}\}$ the time series obtained after one application of the RCMA to the residuals of order $c$, $w_n^{(c)} = v_n/(V v_n^{(1)}...v_n^{(c)})$ and by $\{u_n^{(c+1;2)}\}$ that ob-
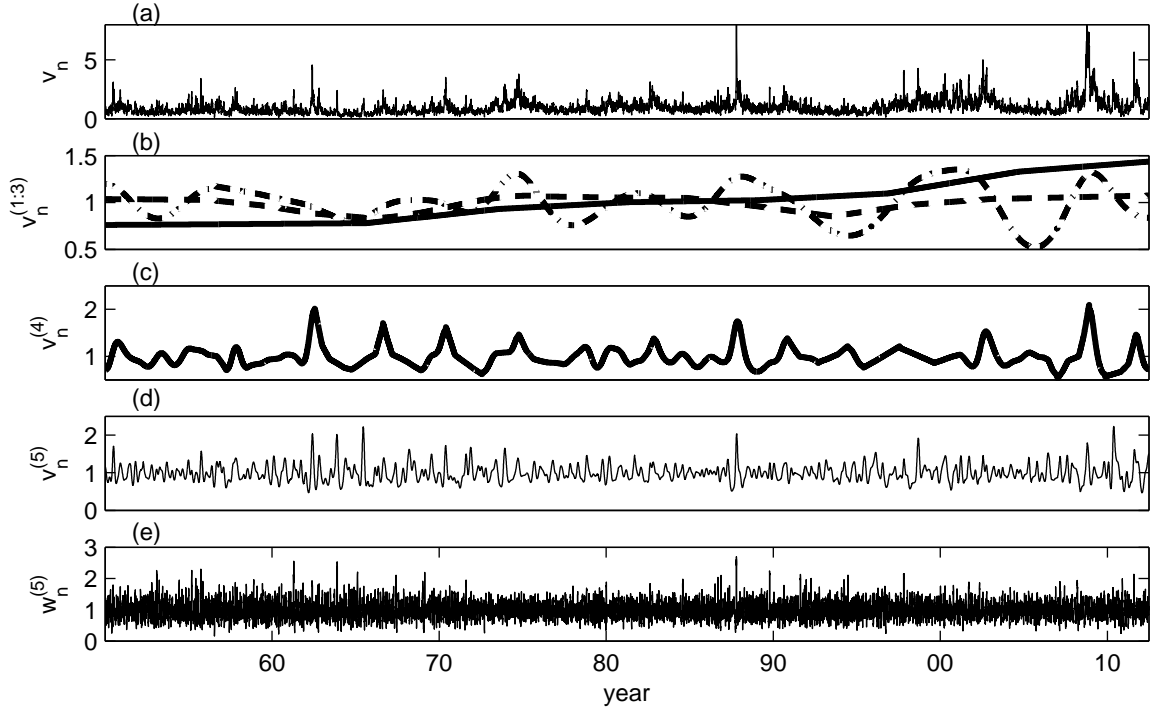
**Fig. 3.** (a) The estimated volatility of the S&P500 index divided by the mean volatility $V$. For a better visibility of the volatility shape, the range of the y-scale is reduced so that the maximum volatility occurring on 19 October 1987 is cut off. (b-e) The intrinsic superstatistical components and the residuals of the estimated volatility.
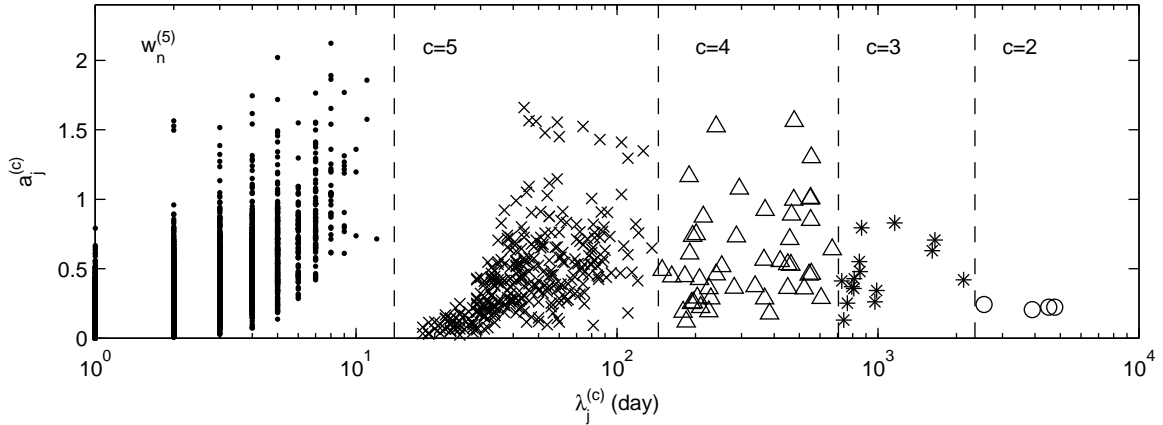


**Fig. 4.** The amplitude $a_j^{(c)}$ equal with the overall variation of the j-th monotonic segment of the $c$ volatility intrinsic superstatistical component as a function of its characteristic time for the S&P500 index. The vertical dashed lines separate the disjoint intervals $I_\lambda^{(c)}$.

tained after a second application to $w_n^{(c)}/u_n^{(c+1;1)}$. It is possible that a single smoothing with the RCMA cannot extract all the variations with the characteristic times in $I_\lambda^{(c+1)}$. We consider that such a situation occurs when the quadratic norm of these subcomponents is not reduced by one order of magnitude $||u_n^{(c+1;2)}||/||u_n^{(c+1;1)}|| > 0.1$. Then we apply once again the RCMA to the new partial residuals $w_n^{(c)}/(u_n^{(c+1;1)} u_n^{(c+1;2)})$. We stop the averagings

after $k$ iterations when the quadratic norm of $u_n^{(c+1;k+1)}$ is one order of magnitude smaller than that of the product $u_n^{(c+1;1)} u_n^{(c+1;2)} ... u_n^{(c+1;k)}$. This procedure is illustrated in the case of the second component in Appendix (Fig. 8).

After several applications of the RCMA, there remain some monotonic segments with reduced lengths and amplitudes which are not related to the characteristic times of the $c+1$ component. A large-scale monotonic variation may be separated into two shorter segments with the same

monotony by a small inflexion with opposite monotony. We replace these three segments by a single monotonic segment with the length equal to the sum of the three lengths using the ACD algorithm designed to determine the monotonic component of an arbitrary time series [20, 22]. In this way the three initial characteristic times are replaced by a single one equal to their sum so that the interval $I_\lambda^{(c+1)}$ is shifted towards the larger values of the characteristic times. We eliminate the small monotonic segments in ascending order of their lengths until $I_\lambda^{(c+1)}$ does not overlap $I_\lambda^{(c)}$. This procedure is also illustrated in the case of the second component in Appendix (Fig. 8).

As stated before, the values of the parameters of the RCMA and the number of the ACD iterations are chosen such that the resulting interval $I_\lambda^{(c+1)}$ has a minimum width and is as close as possible to the previous one. We have used a subjective and empirical procedure to search the optimal parameters so that we have not obtained a unique best solution. But we have strictly respected the condition that the intervals $I_\lambda^{(c)}$ should be disjoint such that the intrinsic character of the volatility components is preserved.

## 4 Volatility intrinsic components

Before applying the adaptive iterative procedure presented in the previous section to identify the intrinsic superstatistical components of the estimated volatility, we need to know the initial largest-scale components. They are determined such that the global shape of the largest-scale component should be preserved (Appendix A) and are plotted in Fig. 3(b). The first component $\{v_n^{(1)}\}$ is monotonic (continuous line) and the second component $\{v_n^{(2)}\}$ has four monotonic segments (dashed line).

The next three intrinsic superstatistical components are obtained with the iterative method described in Sect. 3 taking as reference the interval $I_\lambda^{(2)}$ [Figs. 3(b-d)]. We applied the RCMA algorithm three times with semilengths of the smoothing window $K^{(3)} = 150$, $K^{(4)} = 30$, and $K^{(5)} = 6$ repeated $i^{(3)} = i^{(4)} = i^{(5)} = 3$ times. The ACD algorithm was applied one time, 20 times, and 37 times, respectively. We analyze the spectral properties of the intrinsic components plotting the overall variations of the monotonic segments as a function of their lengths, i.e., their characteristic times (Fig. 4). The first component $\{v_n^{(1)}\}$ is monotonic and has a single characteristic time equal to the time series length (not plotted in Fig. 4).

The third intrinsic component $\{v_n^{(3)}\}$ [point-dashed line in Fig. 3(b)] has the characteristic times ranging from 3 to 8.5 years (asterisks in Fig. 4). The characteristic times of the forth and fifth intrinsic components [Figs. 3(c) and (d)] range between half a year to 2.6 years, and one to six months, respectively (triangles and crosses in Fig. 4). The residuals $w_n^{(5)}$ [Fig. 3(e)] have characteristic times between one and 12 days (point markers in Fig. 4). We have to take into account that the characteristic times shorter than 5
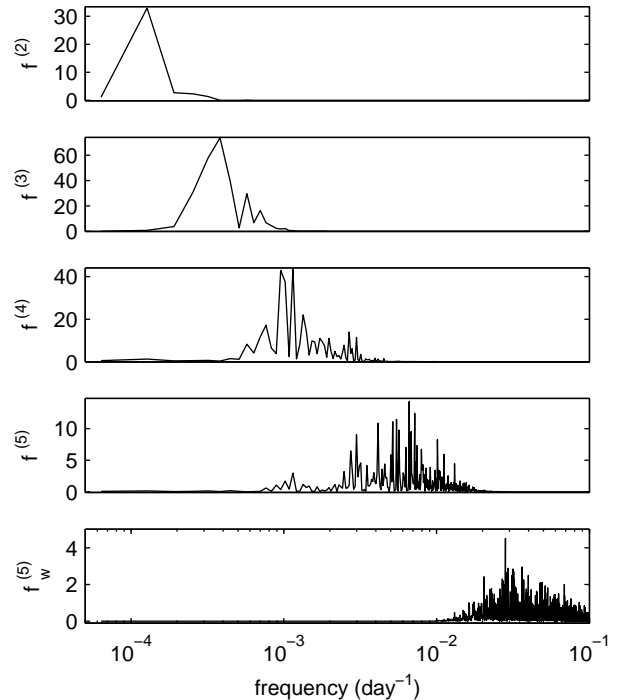


**Fig. 5.** The power spectra of the nonmonotonic intrinsic superstatistical components ($c > 1$) and of the residuals of the estimated volatility of the S&P500 index.

days of $w_n^{(5)}$ are not reliable, because they are mixed with those of the estimated noise in Eq. (2).

The volatility intrinsic components have been determined such that their characteristic times are rigourously disjoint (Fig. 4). As discussed in Sect. 3, there is a possibility that the neighboring intrinsic components may have monotonic variations with overlapping characteristic times. Indeed, there exists a superposition of the Fourier time scales but it is minimal, the regions of the maximum power spectra of the intrinsic components being clearly separated (Fig. 5).

In the following, we use this volatility decomposition to analyze the dynamics at different time scales. We can associate a pdf only to the last two intrinsic components $\{v_n^{(4)}\}$ and $\{v_n^{(5)}\}$. We can also associate a pdf to the residuals of order five $\{w_n^{(5)}\}$. Their pdfs are very similar (Fig. 6) and they are likely realizations of stationary stochastic processes. Because of their resemblance we group them as the random part of the volatility $v_n^{(\text{rand})} = v_n^{(4)} v_n^{(5)} w_n^{(5)}$.

The first two volatility components contain the largest-scales variations and we group them as the deterministic part of the volatility $v_n^{(\text{det})} = v_n^{(1)} v_n^{(2)}$. Even if they were generated by a stochastic process, because of their limited number of values they cannot be distinguished from a deterministic signal. The different nature of these two components from the others is also sustained by their smaller amplitudes of the monotonic segments (Fig. 4).
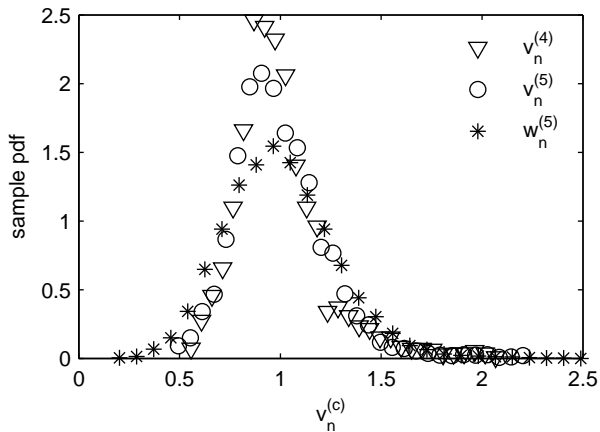
**Fig. 6.** The sample pdfs of the random superstatistical components of the volatility of the S&P500 index and of the residuals of order five.

The shape of the third intrinsic component and its characteristic times can be related to the well-known business cycles [23]. We interpret it as a transition component between the deterministic and random parts. In this way the estimated volatility is split up into a deterministic part and a random part, the third intrinsic component making the transition between them $v_n = v_n^{(\text{det})} v_n^{(3)} v_n^{(\text{rand})}$.

The existence of the deterministic large-scale components means that the volatility is a nonstationary time series [24]. This result supports the alternative approach in quantitative finance, revived in the last decade, which considers that the volatility is not a stochastic process, but a slowly varying deterministic function [25]. Even more similar to our result is the spline-GARCH model in which the volatility is a superposition of a deterministic function and a stationary stochastic process [26].

The existence of the deterministic components also means that there is no unique pdf of the volatility. Because the large-scale components have a deterministic behavior, the global pdf is a discrete summation, not an integral as in Eq. (3) [17,18]. As a consequence, $F(r)$ cannot be computed as a universal expression and it depends on the particular form of the deterministic part. This fact could be a possible explanation for the difficulty to determine a general pdf for the financial time series [27].

## 5 Synchronization of intrinsic volatility components

Now we check if the random intrinsic components of the volatility are independent, as the superstatistical model (3) assumes. We can destroy the possible correlations between the three components of $v_n^{(\text{rand})}$ by shuffling their values and then multiplying them. The majority of the values of the initial and the shuffled pdfs coincide, proving that most of the time the three random intrinsic components fluctuate independently [Fig. 7(a)]. Their tails differ

from each other only for $v_n^{(\text{rand})} > 3$, for 120 values representing 0.76% of all the volatility values. Hence more than 99% of the time the random intrinsic components fluctuate independently and the central part of the resulting pdf can be computed as a multiple integral generalizing Eq. (3).

We have obtained very similar results for other two financial indices. This is not surprising in the case of the DJI index which characterizes the same financial market as the S&P500 index. In Fig. 7(c) we plot the same quantities as those in Fig. 7(a), but for the Nikkei index. In this case the tail of the random part of the volatility and that of the shuffled one differ for 0.99% of their values.

It is well-known that volatility has heavy tails [19]. The question is if the tail of the volatility random part $v_n^{(\text{rand})}$ remains heavy. A pdf with heavy tails has an asymptotic behavior following a power law and its moments of order higher than the absolute value of the exponent are infinite [28]. Because the existing statistical methods to recognize and to measure power law tails have significant errors [28], we compare the volatility tails with the tails of the Laplace distribution $e^{-\mu|x|}/(2\mu)$, where $\mu$ is a positive real parameter. We use this distribution as a reference because, unlike the power law distributions, all its moments are finite although it has heavier tails than the Gaussian distribution.

We need several thousands of observations to establish if a sample pdf has heavy or exponential tails [29], condition satisfied by our volatility time series. We have numerically generated 1000 uncorrelated time series with Laplace distribution of unit variance ($\mu = 1/\sqrt{2}$) having the same length as the volatility time series. Then we have computed the cumulative distribution function (cdf) for each artificial time series and we have established the limits containing 95% of the complementary cdf (1 - cdf) [dashed lines in Figs. 7(b) and (d)]. We have also generated 1000 shuffled versions of $v_n^{(\text{rand})}$, we have standardized them by extracting their mean and then dividing the result by their standard deviation, and we have established the 95% interval of variation of their complementary cdfs [continuous lines in Figs. 7(b) and (d)].

The right tail of the volatility random part $v_n^{(\text{rand})}$ is significantly heavier than those of the Laplace distribution for both indices [Figs. 7(b) and (d)]. This tail is reduced by shuffling, but the tails of the standardized shuffled time series remain almost in all cases heavier than the exponential tails. Hence, even if the random intrinsic components of the volatility were independent, their product would have heavy tails. The correlation between them only enhances their heaviness. In conclusion, the extreme volatility is the result of both the superstatistical mechanism (mixture of different statistics) and the correlation between the random volatility components.

Large volatility occur during financial crashes when the financial markets structure is reorganized and all the categories of investors act in the same way, i.e., they become synchronized [30–32]. Synchronization of dynamically interacting units in a complex network was observed in a large variety of domains [33]. In the case of financial
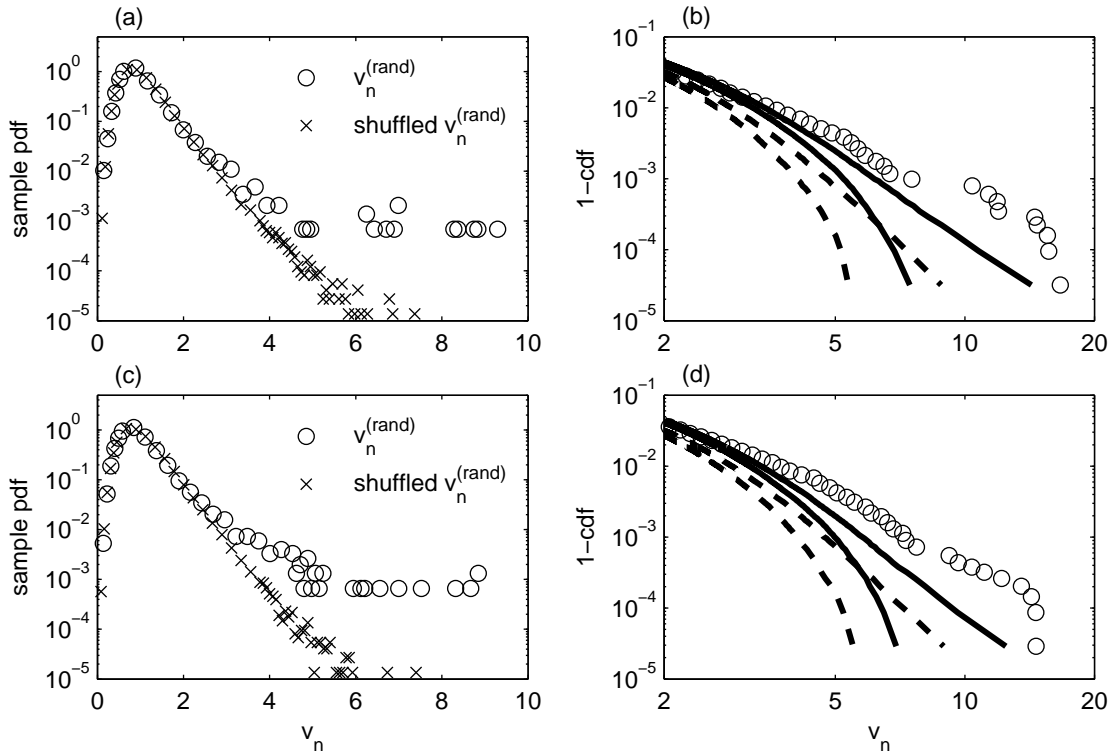
**Fig. 7.** The sample pdf of $v_n^{(\text{rand})}$ and of the product of the shuffled random intrinsic superstatistical components for the S&P500 index (a) and for the Nikkei index (c). The complementary cdf (1-cdf) of the standardized $v_n^{(\text{rand})}$ (circle markers) and the 95% interval of variation of the standardized product of the shuffled random intrinsic components (continuous lines) and of the Laplace distribution (dashed lines) for the S&P500 index (b) and for the Nikkei index (d).

markets we have shown that the synchronization of the network structure is accompanied by the temporal synchronization of the dynamics at different time scales.

# 6 Conclusions

We have shown that the well-separated spectral intrinsic components of the financial volatility allow the search for correlations between the dynamics at different scales. During the financial crashes the random components of the volatility become synchronized generating probability distributions with heavy tails. This behavior is present in the evolution of three different financial indices (S&P500, DJI, and Nikkei).

Generalizing this result we conjecture that the temporal multiscale synchronization of the communities of a complex network may be a general mechanism to generate heavy tails different from those proposed till now as the combination of exponentials, the Yule process, critical phenomena, self-organized criticality [34], the superstatistical model [5] or the mixture of Gaussians [35]. The fact that the volatility heavy tails result from the simultaneous action of two distinct such mechanisms indicates that any of these mechanisms could collaborate to generate heavy tails when the system has a hierarchical complex structure.

In accordance with Eq. (2), the complex structure of the volatility is conveyed to logreturns. The heterogeneity of the intrinsic components and the synchronization of small-scale components might provide an explanation for the difficulty to model the logreturn distribution [27]. In particular, even if the financial returns have a universal tail index around 3 [36], there exist significant variations between individual companies [37]. These variations are small for intraday returns, but they increase for daily returns. The variations are even larger for exchange rates between different currencies [3]. Such variations can be analyzed in relation with the complex evolution of the intrinsic components obtained with the adaptive decomposition algorithm presented here.

There are many possible applications of our adaptive decomposition algorithm due to its ability to separate nonlinear and nonstationary time series into disjoint intrinsic spectral components. They can be analyzed by usual statistical tests and the possible spectral heterogeneities may be discovered.

# A The first two volatility intrinsic components

We determine the first two intrinsic components of the volatility by imposing the condition that the global shape of the largest-scale component should be preserved by applying additional smoothings. In order to obtain a strong
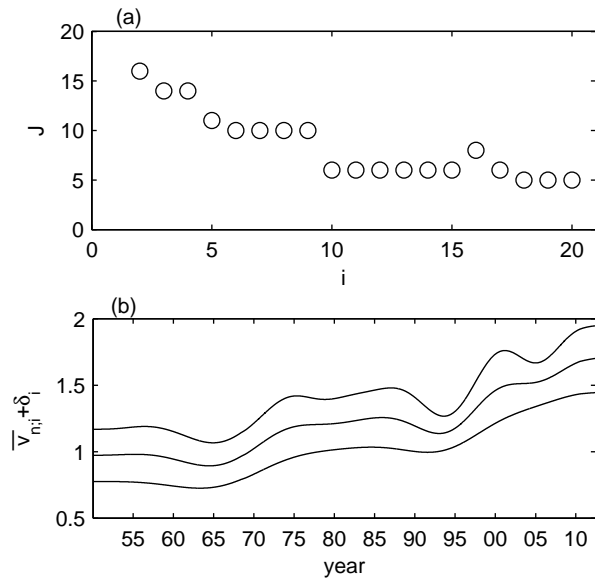
**Fig. 8.** (a) The number of the monotonic segments of the averaged estimated volatility of the S&P500 index as a function of the number of averagings ($i > 1$). (b) The estimated volatility averaged 6, 10, and 18 times. For clarity, the less smoothed time series are displaced by $\delta_6 = 0.4$ and $\delta_{10} = 0.2$, while $\delta_{18} = 0$.

smoothing of the volatility time series we apply the MA (4) with a large value of the averaging window $K = 500$. We repeat the averaging 20 times and for each number of averagings $i$ we compute the number $J$ of monotonic segments of the averaged time series $\{\overline{v}_{n;i}\}$ [Fig. 8(a)]. After the first averaging the number of monotonic segments is reduced from 7842 contained by the initial time series down to 16. The next variations of $J$ occur only at some values of $i$ and are much smaller than the first one.

In Fig. 8(b) we plot three of the averaged time series $\{\overline{v}_{n;i}\}$ corresponding to some of the main jumps of $J$. After $i = 6$ averagings the averaged volatility has $J = 10$ monotonic segments and the shortest of them with 877 business days begins in 1975 and ends at 1978. The next three averagings preserve the number of monotonic segments but the length of the shortest one is reduced to 196 business days and its amplitude decreases. This monotonic segment and that beginning in 2001 and ending at 2004 are simultaneously eliminated by the 10th averaging, so that the number of the monotonic segments becomes $J = 5$. Now the shortest monotonic segment has 1232 business days and is situated at the beginning of the averaged time series. It is eliminated by the 18th averaging after which there remain only 4 monotonic segments. A detailed analysis of the effect of repeated averagings on the local extrema can be found in Chap. 6 of [20].

Additional averagings do not reduce the number of the monotonic segments and therefore we consider that the estimated volatility averaged 18 times describes the largest-scale monotonic variations of the volatility. It contains four time intervals: two with almost constant averaged volatil-
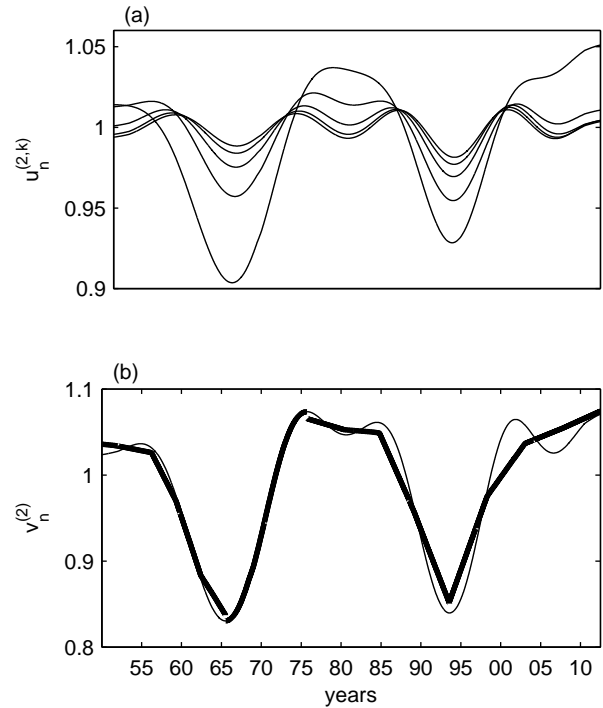


**Fig. 9.** (a) The five partial averages $u_n^{(2;k)}$ of the second intrinsic component of the S&P500 index. (b) The product of the first four partial averages (thin line) and the second intrinsic component (thick line) obtained after three applications of the ACD algorithm.

ity, only slightly decreasing (from 1950 to 1965 and from 1980 to 1995) and two with increasing averaged volatility (1970s and after 1995 to 2012). The global shapes of the averaged volatilities $\{\overline{v}_{n;i}\}$ for $i < 18$ do not significantly differ from each other, except for several fluctuations with small amplitudes.

The averaged volatility $\{\overline{v}_{n;18}\}$ has an obvious global increasing component over which the four monotonic segments described above are superposed [Fig. 8(b)]. This superposition alters the characteristic times, increasing those for the increasing segments and decreasing the others. Therefore, by means of the ACD algorithm [20], we separate the global monotonic component of the averaged volatility and we identify it with the first component $\{v_n^{(1)}\}$ of the volatility [continuous line in Fig. 3(b)].

We may not identify the second volatility intrinsic component with $\overline{v}_{n;18}/v_n^{(1)}$ because we are not sure that we have successfully extracted the most part of the largest-scale variations of the volatility. Therefore we apply the RCMA with $K^{(2)} = 500$ and $i^{(2)} = 18$ several times to the residuals $w_n^{(1)} = v_n/v_n^{(1)}$ (Sect. 3). In Fig. 9(a) we plot the first five partial averages $u_n^{(2;k)}$ and we observe that their amplitudes progressively diminish with $k$, while preserving approximately the same shape. We neglect the fifth partial average and we retain only the first four partial averages because $||u_n^{(2;5)}||/||u_n^{(2;1)}...u_n^{(2;4)}|| = 0.095$.

Finally, we eliminate by means of the ACD algorithm the insignificant monotonic segments from the product $u_n^{(2;1)}...u_n^{(2;4)}$. The shortest monotonic segment has 973 business days and lasts from 1980 to 1984 [Fig. 9(b)]. After its elimination, the resulting decreasing segment has 4409 business days. The second monotonic segment which we eliminate has 1195 business days and lasts from 2001 to 2006 and the resulting increasing segment has 4761 business days. Finally, the third eliminated monotonic segment lays at the left boundary of the time series and then the ACD algorithm is applied only to two neighboring monotonic segments. By applying the ACD algorithm, the number of the monotonic segments diminishes from 9 to 4 and their lengths range between 10 and 19 years. The final result is the second intrinsic component $\{v_n^{(2)}\}$ [the dashed line in Fig. 3(b) or the thick line in Fig. 9(b)].

# References

1. L.F. Costa, O.N. Oliveira, G. Travieso, F.A. Rodrigues, P.R.V. Boas, L. Antiqueira, M.P. Viana, and L.E.C. da Rocha, Adv. Phys. **60**, 329 (2011).
2. A.L. Barabási, E. Ravasz, and Z. Oltvai, in *Statistical Mechanics of Complex Networks*, edited by R. Pastoras-Satorras, M. Rubi, and A. Diaz-Guilera (Springer, Berlin, 2003).
3. M.M. Dacorogna, R. Gençay, U.A. Müller, R.B. Olsen, and O.V. Pictet, *An Introduction to High-Frequency Finance* (Academic Press, San Diego, 2001).
4. R.S. Tsay, *Analysis of Financial Time Series* (Wiley, Hoboken, 2010).
5. C. Beck and E.G.D. Cohen, Physica A **322**, 267 (2003).
6. C. Beck, Phil. Trans. R. Soc. A **369**, 453 (2011).
7. D.N. Sob'yanin, Phys, Rev. E **84**, 051128 (2011).
8. C. Beck, Braz. J. Phys. **39**, 357 (2009).
9. C. Beck, Phys. Rev. Lett. **98**, 064502 (2007).
10. J. Gao, Y. Cao, W. Tung, and J. Hu, *Multiscale Analysis of Complex Time Series* (Wiley, Hoboken, 2007).
11. D.B. Percival and A.T. Walden, *Wavelet Methods for Time Series Analysis* (Cambridge, Cambridge, 2000).
12. N.E. Huang, Z. Shen, S.R. Long, M.C. Wu, H.H. Shih, Q. Zheng, N.C. Yen, C.C. Tung, and H.H. Liu, Proc. R. Soc. Lond. A **454**, 903 (1998).
13. R. Cont, Quant. Financ. **1**, 223 (2001).
14. S.J. Taylor, *Asset Price Dynamics, Volatility, and Prediction* (Princeton University Press, Princeton, 2007).
15. E. Van der Straeten and C. Beck, Phys. Rev. E **80**, 036108 (2009).
16. A. Gerig, J. Vicente, and M.A. Fuentes, Phys. Rev. E **80**, 065102 (2009).
17. C. Vamoş and M. Crăciun, Phys. Rev. E **81**, 051125 (2010).
18. C. Vamoş and M. Crăciun, Eur. Phys. J. B **86**, 166 (2013).
19. Y. Liu, P. Gopikrishnan, P. Cizeau, M. Meyer, C.-K. Peng, and H.E. Stanley, Phys. Rev. E **60**, 1390 (1999).
20. C. Vamoş and M. Crăciun, *Automatic Trend Estimation* (Springer, Dordrecht, 2012).
21. P. Chaudhuri and J.S. Marron, J. Am. Stat. Assoc. **94**, 807 (1999).
22. C. Vamoş, Phys. Rev. E **75**, 036705 (2007).
23. J.A. Schumpeter, *Business Cycles. A Theoretical, Historical and Statistical Analysis of the Capitalist Process* (McGraw-Hill, New York, 1939).
24. P.J. Brockwell, R.A. Davies, *Time Series: Theory and Methods* (Springer Verlag, New York, 1996).
25. S. Van Bellegem, in *Wiley Handbook in Financial Engineering and Econometrics: Volatility Models and Their Applications*, edited by L. Bauwens, C. Hafner, S. Laurent (Wiley, New York, 2011).
26. R.F. Engle, J.G. Rangel, Rev. Financ. Stud. **21**, 1187 (2008).
27. J. Voit, *The Statistical Mechanics of Financial Markets* (Springer, Berlin, 2005).
28. S.I. Resnick, *Heavy tails Phenomena. Probabilistic and Statistical Modeling* (Springer, New York, 2007).
29. C.C. Heyde and S.G. Kou, Oper. Res. Lett. **32**, 399 (2004).
30. J.P. Onnela, A. Chakraborti, K. Kaski, J. Kertész, and A. Kanto, Phys. Rev. E **68**, 056110 (2003).
31. M. McDonald, O. Suleman, S. Williams, S. Howison, and N.F. Johnson, Phys. Rev. E **77**, 046110 (2008).
32. T.K.D. Peron and F.A. Rodrigues, Europhys. Lett. **96**, 48004 (2011).
33. A. Arenas, A. Díaz-Guilera, J. Kurths, Y. Moreno, and C. Zhou, Phys. Rep. **469**, 93 (2008).
34. M.E.J. Newman, Contemp. Phys. **46**, 323 (2005).
35. S. Gheorghiu and M.-O. Coppens, PNAS **101**, 15852 (2004).
36. P. Gopikrishnan, V. Plerou, L.A.N. Amaral, M. Meyer, and H.E. Stanley, Phys. Rev. E **60**, 5305 (1999).
37. V. Plerou, P. Gopikrishnan, L.A.N. Amaral, M. Meyer, and H.E. Stanley, Phys. Rev. E **60**, 6519 (1999).